PCCP

Accepted Manuscript

This is an *Accepted Manuscript*, which has been through the Royal Society of Chemistry peer review process and has been accepted for publication.

Accepted Manuscripts are published online shortly after acceptance, before technical editing, formatting and proof reading. Using this free service, authors can make their results available to the community, in citable form, before we publish the edited article. We will replace this *Accepted Manuscript* with the edited and formatted *Advance Article* as soon as it is available.

You can find more information about *Accepted Manuscripts* in the **Information for Authors**.

Please note that technical editing may introduce minor changes to the text and/or graphics, which may alter content. The journal's standard **Terms & Conditions** and the **Ethical guidelines** still apply. In no event shall the Royal Society of Chemistry be held responsible for any errors or omissions in this *Accepted Manuscript* or any consequences arising from the use of any information it contains.

Please do not adjust margins

Journal Name

ARTICLE

The Roles of Different Titanium Species in TS-1 zeolite on Propylene Epoxidation Studied by In Situ UV Raman Spectroscopy

Guang Xiong,*[a] Yuanyuan Cao,[b] Zhendong Guo,[a] Qianying Jia,[a] Fuping Tian,[a] and Liping liu[a]

Titanium silicalite (TS-1) zeolites with the different titanium species were synthesized and characterized by ultraviolet (UV)-Raman, ultraviolet visible (UV-Vis) absorption spectroscopies and NH_3 temperature programmed desorption (NH_3-TPD) method. The role of different titanium species in TS-1 samples has been investigated by gas chromatography-Raman spectrometry (GC-Raman) during the propylene epoxidation process. For the first time, a positive correlation was found among the concentration of framework Ti species, the amount of active intermediate Ti-OOH (η^2) and the conversion of propylene by in-situ GC-Raman technique. The results give evidence that the framework titanium species is the active center and Ti-OOH (η^2) is the active intermediate. The presence of extra-framework Ti species is harmful to propylene epoxidation. Furthermore, the amorphous Ti species has more negative effect on the yield of propylene oxide (PO) than the anatase TiO_2. The NH_3-TPD results reveal that the amorphous Ti species are more acidic thus should be mainly responsible for the further conversion of PO.

Introduction

Titanium silicalite (TS-1) has received considerable interest during the last decade because of its unique catalytic properties in oxidation reactions under mild conditions, especially with the use of hydrogen peroxide (H_2O_2) as the oxidant.[1–3] It was accepted that there are several types of titanium species in TS-1 zeolite:[2] the isolated titanium species in the framework, the amorphous Ti species and the anatase TiO_2. It is commonly believed that the isolated titanium species in the framework of the TS-1 zeolite is the active center for the selective oxidation and the anatase TiO_2 can decompose H_2O_2.[4] However, the role of the amorphous Ti species in the epoxidation reactions is still debated. Several coordinated structures of the amorphous Ti species have been proposed:

(1) the hexacoordinated species with two water molecules in the coordination sphere;[5] (2) a totally symmetric vibration of hexacoordinated Ti-O-Ti linkages;[6–9] and (3) the isolated single-bonded TiO_x species attached to the zeolite lattice.[10] Different synthetic methods may result in the formation of the different titanium species, which increases the complexity of the research. Therefore, a systematic study on the function of the different titanium species in titanium silicalite (TS-1) is required.

Raman spectroscopy is considered as one of the powerful tools for characterizing catalysts and reagents, particularly under reaction conditions.[11] It has been proved to be a useful tool to characterize different titanium species in TS-1. The isolated tetrahedral titanium species in the framework exhibits three resonance enhanced Raman bands at 490, 530, and 1125 cm^{-1} with the use of a 244 nm laser line. These bands are related to the [TiO_4] units in the lattice.[12–14] Recently, an enhanced Raman band at 700 cm^{-1} was assigned to the

[a] State Key Laboratory of Fine Chemicals, School of Chemical Engineering, Dalian University of Technology, Dalian 116012, China Fax: (+86) -411-84986340 E-mail: gxiong@dlut.edu.cn
[b] Daqing Chemical Research Center, CNPC, Daqing 163714 China.

Ti−O−Ti linkages of the non-framework amorphous Ti species.[9] In the spectra excited by 325 and 532 nm lines, the bands at 144, 395, and 637 cm^{-1} are ascribed to non-framework anatase TiO_2.[13] Many experimental approaches (XANES,[15-17] EXAFS,[18-21] FT-IR[22,23] and Raman spectroscopy[24]) and computer calculations[20,25-28] have also been used for the investigation of the TS-1/H_2O_2/H_2O system. The reaction intermediates for propylene epoxidation have also been studied by in situ UV Raman spectroscopy systematically. In our previous study a feature at 837 cm^{-1}, which has been assigned to the O−O stretching mode in the Ti−OOH (η^2) species, has been found active in the propylene epoxidation.[24] In addition, UV-Vis spectroscopy is the other most-used method for characterizing the structure of titanosilicate,[29] especially for TS-1 zeolite. Three UV-Vis absorption bands (190–210, 270–280, and 320 nm) indicate the existence of framework Ti species, amorphous Ti species and anatase TiO_2.

Although some efforts have been done to elucidate the function of the different titanium species in TS-1, the functions of different titanium species and the types of active intermediates are still debatable.[30,31] Thus, a study on the typical TS-1 samples (containing different titanium species) under reaction condition are highly required for a deeper understanding of the active/non-active titanium sites and reaction intermediates. In this study, TS-1 zeolites containing different titanium species were synthesized by changing the Ti/Si ratio and synthesis conditions. Then gas chromatography-Raman spectrometry (GC-Raman) was used to investigate the reaction intermediates on the TS-1 and the products for propylene epoxidation. The roles of the different titanium species in TS-1 are discussed. Particular attention has been paid to the effect of amorphous Ti species on propylene epoxidation.

Experimental

Synthesis:

The TS-1 molecular sieve was synthesized hydrothermally by a conventional procedure according to the literature.[32] Chemical reagents include tetrabutylorthotitanate (98%, Kefeng chemical reagent Co.,Ltd., Shanghai), tetraethyl orthosilicate (AR, Westlong Chemical Plant, Shantou), isopropyl alcohol (AR, Fuyu FineChemical Co., Ltd., Tianjin), and tetrapropyl ammonium hydroxide (TPAOH, synthesized according to the literature, 1.23 M[33]). The titanium source and silicon source were hydrolyzed in TPAOH solution at 298 K, respectively. After being hydrolyzed for 6 h, the two solutions were mixed together and then the gel was crystallized at 443 K for 72 h. Finally, the sample was calcined at 813 K for 6 h to remove the template. The molar composition is 1.0 SiO_2: (0.0125-0.033) TiO_2: 0.3 TPAOH: 1.0 IPA: 30 H_2O.

Characterization

The UV−Vis spectra were recorded on a SHIMADZU UV-240 spectrometer using $BaSO_4$ as a reference. The PeakFit (4.12) program for curve fitting was used to analyze the overlapped absorption bands.

UV-Raman spectra were recorded on a DL-2 Raman spectrometer, with a collection time of 300 s. A 244 nm line of LEXEL LASER was used as the excitation sources. The laser power at the sample was less than 5 mw. An Acton triple monochromator was used as a spectrometer for Raman

Journal Name ARTICLE

scattering. The spectra were collected by a Prinston CCD detector. During the in situ experiments, the pellet of the TS-1 sample (0.05 g) was moved into a stainless steel cell equipped with a quartz window after dropping $H_2O_2/H_2O/CH_3OH$ solution. Propylene (3% propylene and 97% helium gas in volume fraction) was introduced into the cell at a flow rate of 25 mL/min. The spectra during the reaction process were recorded by the UV Raman spectrometer. Meanwhile, the component analysis of the output gas was performed on a GC 9790 gas chromatograph, using a flame ionization detector and a capillary column (PEG-20M, 30 m). The concentration of propylene oxide was represented directly by its peak area in the GC spectra. The peak area was integrated by the OriginPro (8.5.1) program.

The NH_3 temperature programmed desorption (NH_3-TPD) was performed by using ChemBET 3000 chemisorb instrument from Quantachrome. The effluent stream was monitored continuously with a thermal conductivity detector to determine the rate of ammonia desorption.

Results and Discussion

TS-1 with different SiO_2/TiO_2 ratios

UV–Vis spectra of the TS-1 zeolites with different titanium contents are shown in Fig. 1. A strong peak at 210-225 nm appears in the spectra, indicating the presence of the framework titanium species in all the samples. It is clear that the relative intensity of the 210-225 nm band increases with decreasing the SiO_2/TiO_2 ratio. As for the TS-1-30, it can be seen that the band assigned to framework titanium species is shifted from 210 nm to 225 nm. The shift of the framework

titanium absorption maximum to higher wavelength may be due to the loosely coordinated surrounding Si–O bands. This implies that the local coordinated environment of the framework titanium species in TS-1-30 is slightly different from those in TS-1-80 and TS-1-50.[5] The intensity of the absorption band at 270 nm, which is assigned to the amorphous Ti species,
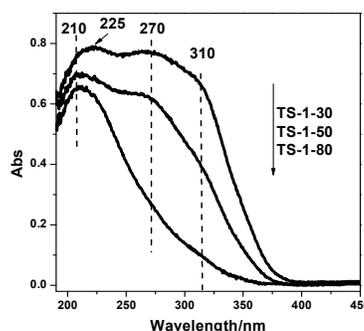
Fig. 1 UV-Vis spectra of the TS-1 samples with different SiO_2/TiO_2 ratios.
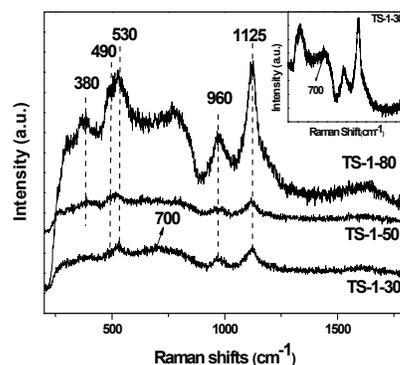
Fig. 2 UV-Raman spectra of the TS-1 samples with different SiO_2/TiO_2 ratios (244 nm).

also increases with decreasing the SiO_2/TiO_2 ratio. The absorption band at 310 nm, which corresponds to the non-

framework anatase TiO_2, is very weak in the spectrum of TS-1-80. The intensity of the band increases with decreasing the SiO_2/TiO_2 ratio. Although the contents of all three titanium species increase as the amount of the starting titanium source increases, the concentration of the non-framework titanium species has a more obvious change.

Fig. 2 shows the Raman spectra of the TS-1 with different titanium contents collected with a 244 nm laser line. Compared with those of the TS-1-80, the intensities of all the peaks of the samples TS-1-50 and TS-1-30 are obviously weak, which is due to the strong absorption of UV light by non-framework Ti species. The peaks at 380, 490, 530, 700, 800, 960, and 1125 cm^{-1} are observed in the spectra. The peaks at 380 cm^{-1} and 800 cm^{-1} are characteristic of Silicalite-1 zeolite. The 960 cm^{-1} has been assigned to titanyl group Ti=O,[8, 36] Ti-O stretching, silanol group Si-OH, titanium related defect sites[10] or Ti-O-Si bridge.[8] The 490, 530 and 1125 cm^{-1} bands are the characteristics of the framework titanium species in TS-1,[13] while the band at 700 cm^{-1} is assigned to the amorphous Ti species in TS-1.[9] As shown in Fig. 1, increasing Ti content in synthetic gel leads to an increase in the amount of the amorphous Ti species in TS-1. Accordingly, the Raman feature at 700 cm^{-1}, which is closely related to the UV-Vis band at 260-280 nm, appears in the spectra of TS-1-30 and TS-1-50.

Fig. 3 shows NH_3-TPD curves of the TS-1 with different titanium contents. Evidently, the desorption peak of the TS-1-50 at low temperature is larger than that of TS-1-80. This indicates that the TS-1-50 has more weak acid sites than the TS-1-80. It can be seen that the desorption temperature for TS-1-30 in the low temperature range is higher than those for the

other samples, indicating that the acidic strength of weak acid sites on TS-1-30 is stronger than those on the samples with higher SiO_2/TiO_2 ratios. The TS-1-30 and TS-1-50 show the desorption peak at higher temperature, indicating the presence of strong acid sites on both samples. The intensity of the peak for TS-1-30 is higher than that for TS-1-50. Obviously, more strong acid sites are formed as the SiO_2/TiO_2 ratio decreases. As shown in Fig. 1 the titanium-rich samples have more amorphous Ti species and anatase TiO_2. Therefore, there might be a close correlation between the non-framework Ti species and the acidity.
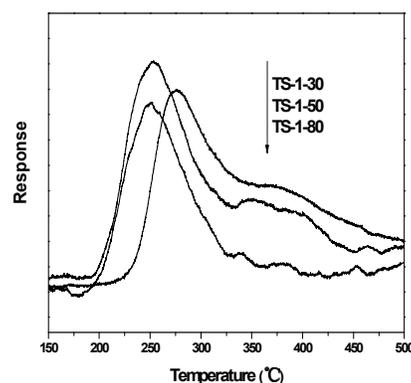
Fig. 3 NH_3-TPD profiles of the TS-1 samples with different SiO_2/TiO_2 ratios.

After dropping 30 µL of $H_2O_2/H_2O/CH_3OH$ solution (the volume ratio of H_2O_2 and CH_3OH in the solvent is 1:1) on the TS-1 sample pellet (0.05 g), the Raman spectra of the TS-1 (SiO_2/TiO_2 ratio 30, 50, 80)/$H_2O_2/H_2O/CH_3OH$ system under a continuous flow of propylene are collected and shown in Fig. 4. The corresponding GC results and intensity of the 837 cm^{-1} peak are shown in Fig. 5. Methanol was added because it is the

Journal Name ARTICLE

best solvent for liquid phase epoxidation of alkenes. It can be seen that the evolution of the Raman spectra of the TS-$1/H_2O_2/H_2O/CH_3OH$ system with different titanium contents are similar. At the beginning of the reaction, the bands at 490, 530, and 1125 cm^{-1} are seriously quenched immediately. The bands at 960 and 1125 cm^{-1} shift to 990 and 1134 cm^{-1}, which has been attributed to the expansion of the Ti coordination sphere.[23] Once the Ti coordination sphere expands, the Td-like symmetry of Ti (IV) species is destroyed, and the symmetry of the vibrational modes is no longer the same as that of the LMCT.[24] A new band at 600 cm^{-1} is attributed to the Ti−O stretching mode in the Ti−O−CH$_3$ moiety,[34] and its appearance gives evidence that the solvent molecule (CH$_3$OH) bonds directly to the Ti center.[15, 17, 35, 36]
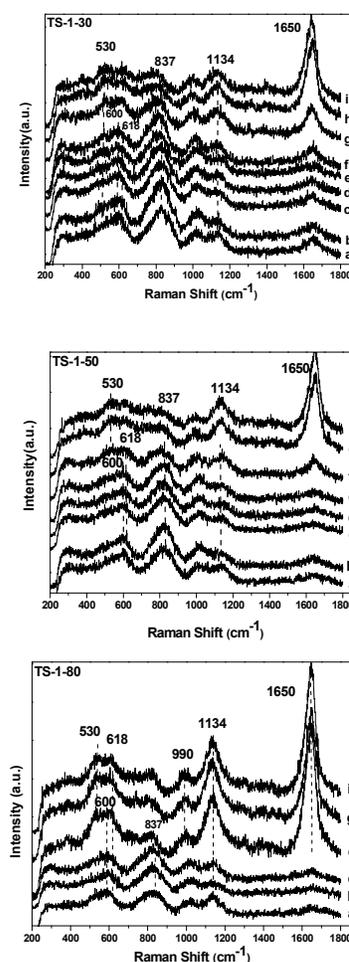
Fig. 4 In situ Raman spectra of the TS-1 (SiO$_2$/TiO$_2$ ratio = 30, 50, 80)/H$_2$O$_2$/H$_2$O/CH$_3$OH system obtained at different times during the methanol-included epoxidation reaction, collected with a 244 nm laser: (a) Raman spectrum obtained at the 6th minute, (b) 12th minute, (c) 18th minute, (d) 25th minute, (e) 32th minute, (f) 38th minute, (g) 46th minute, (h) 54th minute and (i) 60th minute.

Moreover, a shoulder at 618 cm^{-1} has been assigned to the symmetric breathing mode of the Ti(O$_2$) cycle. The feature at 837 cm^{-1}, which has been assigned to a Ti−OOH (η^2) species, appears quickly. The band intensity is obviously influenced by
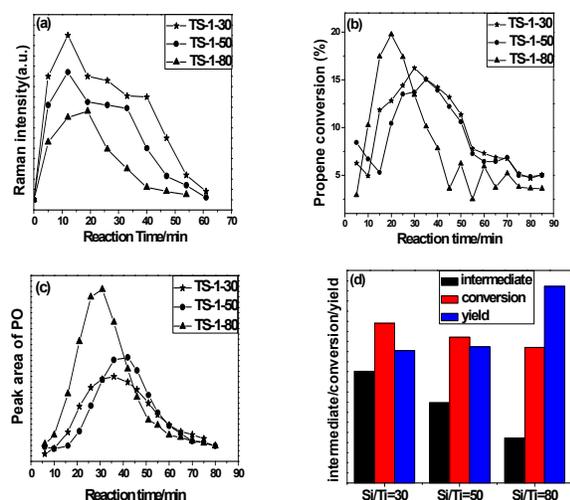
Fig. 5 (A) Raman intensity of the 837 cm^{-1} band (B) the propylene conversion and (C) Peak area of propene oxide in the GC spectra obtained at different times during the epoxidation reaction on the TS-1 with different SiO_2/TiO_2 ratios.

the continuous introduction of propylene. The intensity of the band at 837 cm^{-1} firstly increases, then drops gradually as the time continues. Meanwhile, the peak area of propylene oxide in GC spectra shows the same trend. This implies that the reaction intermediates Ti–OOH (η^2) species were gradually consumed by contacting with the propylene. With the disappearance of the 837 cm^{-1} band, a band at 1650 cm^{-1} which corresponds to propylene physisorbed into the zeolite channels appears. Its intensity increases with increasing the reaction time.

A more important information in the spectra is the difference in the intensity of the band at 837 cm^{-1} as shown in Fig. 5A. The intensity of the band at 837 cm^{-1} decreases in the following order: TS-1(SiO_2/TiO_2 ratio = 30), TS-1 (SiO_2/TiO_2 ratio = 50) and TS-1 (SiO_2/TiO_2 ratio = 80). The UV–Vis spectra

in Fig. 1 show that the intensity of the 210-225 nm band increases with decreasing the SiO_2/TiO_2 ratio. Combined the above results there is a good correlation between the intensities of 210-225 nm peak and the 837 cm^{-1} band, which means that the more the framework Ti species in the TS-1 the higher the concentration of the reaction intermediate Ti–OOH (η^2). This result agrees that the isolated titanium species in the framework of the TS-1 zeolite is the active center for the selective oxidation. Figures 5B and 5C show the propylene conversion and the amount of the produced propylene oxide as the reaction time increases. The integrated peak areas are shown in Fig. 5D. The propylene conversion, which shows the same trend as the amount of the reaction intermediate Ti–OOH (η^2), decreases in the following order: TS-1(SiO_2/TiO_2 ratio = 30), TS-1 (SiO_2/TiO_2 ratio = 50) and TS-1 (SiO_2/TiO_2 ratio = 80). Surprisingly, the amount of the produced propylene oxide is inversely correlated with the propylene conversion. The inverse relationship should be due to the presence of the non-framework amorphous Ti species or anatase TiO_2 on TS-1-30 and TS-1-50. (See Fig. 1) This confirms that more framework titanium species can obtain higher conversion rate of PE, but the non-framework Ti species can convert the PO to other by-products.

TS-1 with different types of non-framework Ti species

Fig. 6 shows the UV–Vis spectra of two TS-1 samples with the SiO_2/TiO_2 ratio = 50. Obviously, the titanium distributions of TS-1-50A and TS-1-50B are different. The TS-1-50A exhibits the absorptions at 212 nm and 270 nm, indicating the formation of the framework and amorphous Ti species. TS-1-

50B, however, shows the strong absorption band at 212 nm
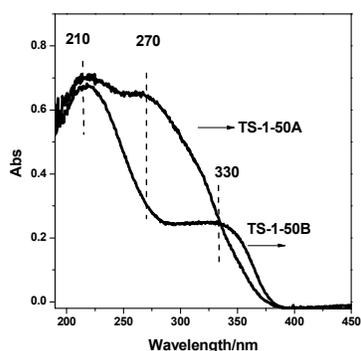
and a

Fig. 6 UV-Vis spectra of the TS-1 samples with SiO_2/TiO_2 ratio = 50.
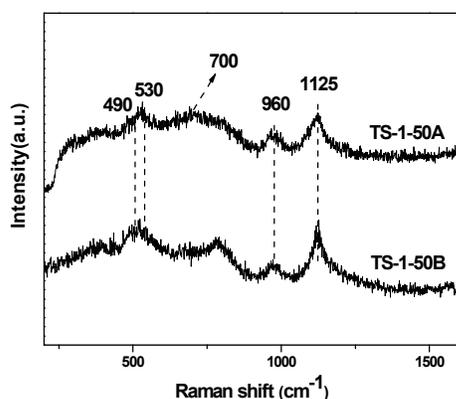
Fig. 7 UV Raman spectra of the TS-1 samples with SiO_2/TiO_2 ratio = 50 (244 nm).
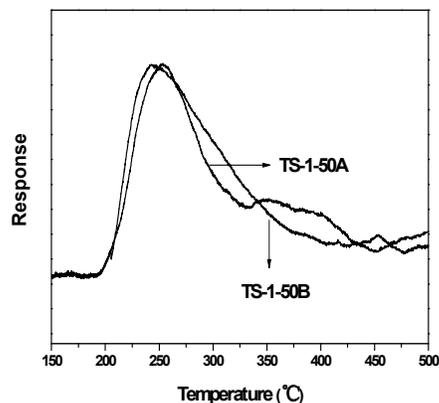
Fig. 8 NH_3-TPD profiles of the TS-1 samples with SiO_2/TiO_2 ratio = 50.

relatively weak band at 330 nm, suggesting the presence of the framework Ti species and the anatase TiO_2. For the two samples the intensities of the band at 220 nm are very close, but the types of the non-framework titanium species are different.

The Raman spectra of the samples with the SiO_2/TiO_2 ratio = 50 are provided in Fig. 7. The bands at 490, 530 and 1125 cm^{-1} are observed for the two samples, suggesting that both samples contain framework titanium species. TS-1-50A exhibits the band at 700 cm^{-1}, which is assigned to the amorphous Ti species. Combined with the UV-Vis results, it can be concluded that the TS-1-50A contains framework titanium and non-framework amorphous Ti species, while the TS-1-50B contains framework titanium and non-framework anatase TiO_2.

Fig. 8 exhibits the NH_3-TPD profiles of the TS-1-50A and TS-1-50B. The desorption peak of the TS-1-50A in the low temperature range is similar to that of TS-1-50B. However,

ARTICLE   **Journal Name**

compared with TS-1-50B, TS-1-50A shows a more obvious desorption peak in the high-temperature region. Combining the results in Fig. 6 and 7, the amorphous Ti species should be responsible for the enhanced acidity. This result is well agreed with the study on the TS-1 acidity characterized by the Hammett indicator titration method.[33] It was found that the acid strength of the TS-1 is $+3.3 < H_0 \leqslant +4.8$. The weaker acid sites, $+3.85 < H_0 \leqslant +4.8$, are due to the framework Ti of TS-1. The stronger acid sites, $+3.3 < H_0 \leqslant +3.85$, are due to the amorphous Ti species. Thus, the amorphous Ti species play an essential role in enhancing the acidity of TS-1.[9]

Although it was reported that the anatase TiO_2 can decompose H_2O_2,[38] the NH_3-TPD result proved that the acidity
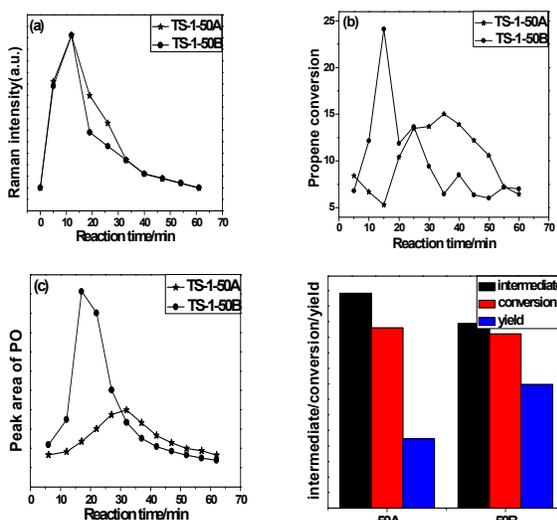
Fig. 9 (A) Raman intensity of the 837 cm^{-1} band (B) the propylene conversion and (C) Peak area of propene oxide in the GC spectra obtained at different times during the epoxidation reaction on the TS-1 with SiO_2/TiO_2 ratio = 50.

of anatase is relatively weak as compared to that of the amorphous TiO_2.[9] In order to clarify the role of the amorphous

TiO_2 and anatase TiO_2, TS-1-50A and TS-1-50B were chosen as the model catalysts for the UV Raman-GC experiment. The Raman spectra of the TS-1-50A and TS-1-50B in $H_2O_2/H_2O/CH_3OH$ system under a continuous flow of propylene are collected and shown in Fig. S1. The corresponding GC results and intensity of the 837 cm^{-1} peak are shown in Fig. 9. The Figure S1 shows that the peak at 837 cm^{-1} appears from the beginning, its intensity gradually increases and finally decreases due to the reaction between the Ti–OOH (η^2) species and propylene. Fig. 9 shows that TS-1-50A produces slightly higher amount of the reaction intermediate for propylene epoxidation than TS-1-50B. This is consistent with the result in Fig. 6, which shows that the absorption at 210 nm of TS-1-50A is slightly higher than that of TS-1-50B. This confirms that the framework Ti species is responsible for the formation of reaction intermediate Ti-OOH (η^2). The propene conversion also shows the same trend. However, the amount of the produced propylene oxide on TS-1-50A is much less than that on TS-1-50B. The amorphous Ti species on the TS-1-50A may account for the bad performance in the propylene epoxidation due to its acidic property.

In order to further prove the role of anatase TiO_2, TS-1-50B and TS-1-60B, which both contain framework titanium and non-framework TiO_2 (anatase), were chosen as the model catalysts for the UV Raman-GC experiment. Fig. 10 shows the UV-Vis spectra of the TS-1-50B and TS-1-60B. The UV-Vis spectra show the strong absorption band at 212 nm and a relatively weak band at 330 nm, suggesting the presence of the framework Ti species and the anatase TiO_2. In this case, curve fitting method is used to accurately evaluate the amount of the framework titanium species and anatase TiO_2. The peak

area ratio (215 nm) of the samples TS-1-50B and TS-1-60B is 1.08, while their peak area ratio (320 nm) is 1.10. Evidently, both the peak areas (215 and 320 nm) of the TS-1-50B are larger than those of
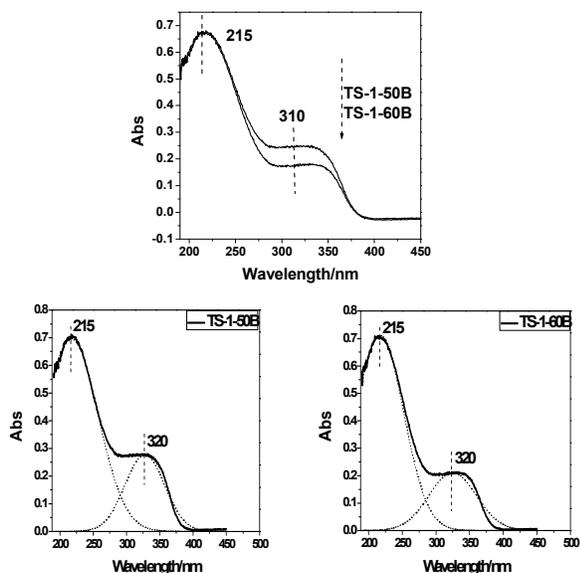
Fig. 10 The UV-Vis spectra of the TS-1 samples.
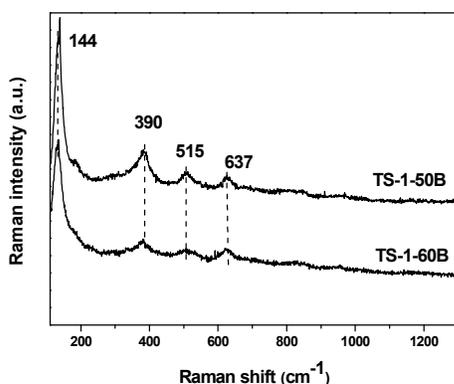
Fig. 11 UV Raman spectra of the TS-1 samples (325 nm)

TS-1-60B, indicating that the TS-1-50B has more framework titanium species and anatase TiO_2 than the TS-1-60B. This is also confirmed by the Raman spectra collected with a 325 nm

laser line (See Fig. 11). The 144, 390, 515 and 637 cm^{-1} bands are the characteristics of the anatase TiO_2 species in TS-1.[13] The intensities of all the peaks of the sample TS-1-50B are obviously higher than those of TS-1-60B, which is well agreed with the UV-Vis result.

The Raman spectra of the TS-1-50B and TS-1-60B in $H_2O_2/H_2O/CH_3OH$ system under a continuous flow of propylene are shown in Fig. S2. Fig. 12 shows that TS-1-50B produces higher amount of reaction intermediates than TS-1-60B. TS-1-50B shows higher propylene conversion but slightly lower amount of propylene oxide than TS-1-60B. This confirms that the framework Ti species is selective for the oxidation of propylene to propylene epoxide. However, the anatase TiO_2 species has a negative effect on the production of propene oxide.

The reaction mechanism of the HPPO process (propene oxide production via hydrogen peroxide) has been studied extensively.[39] As shown in Scheme 1, the first step is the formation of PO through the reaction of propylene with H_2O_2. Then the ring-opening reactions occur by the interaction of PO with either water or methanol, leading to the production of propylene glycol (PG) or methoxy propanol (PGME). They are the two major byproducts, although further reactions between PO and PG/PGME may produce dimmers or heavier adducts. The above results confirm that the framework Ti species is the active sites for the production of PO, since the propylene conversion has positive correlation with the amount of the framework Ti species (UV adsorption at 210 nm). A good correlation was also found between the concentration of the framework Ti species and the amount of Ti-OOH (η^2)

ARTICLE

Journal Name

intermediates (Raman band at 837 cm^{-1}), suggesting that the formation of PO from propylene occurs via a six-coordinated Ti-OOH (η^2) intermediate. The in situ Raman-GC experiment was also performed on anatase TiO_2 to study the role of the anatase TiO_2. Neither the reaction intermediates nor the propylene oxide had been observed, which strongly proves that the propylene epoxidation reaction cannot occur without the framework Ti species. The above results also show that the

Scheme 1 The effect of the amorphous Ti species in propylene epoxidation.

presence of the non-framework Ti species (amorphous TiO_2 and anatase TiO_2) reduces the yield of PO. It can be concluded that the non-framework Ti species are responsible for converting the propylene epoxide to other side products and thereby decrease the epoxide yield. Compared with the anatase TiO_2, the amorphous Ti species on TS-1 is more acidic, thus particularly active for the ring-opening reaction of PO.

Conclusion

The TS-1 zeolites with different Ti distributions were synthesized by hydrothermal method. The reaction intermediates, conversion and the production of PO on the TS-1 were investigated by in situ UV Raman-GC techniques. It reveals that the amount of the framework Ti species in the TS-1 (UV adsorption at 210 nm) is positive related to the formation of the reaction intermediate Ti-OOH (η^2) and propylene conversion. However, the yield of PO is not directly correlated with the amount of Ti-OOH (η^2) if the non-framework Ti species is present. It can be concluded that the framework Ti species in TS-1 is the active site for propylene epoxidation, while the non-framework Ti species should be responsible for the further conversion of propylene oxide. The amorphous TiO_2 species, which is more acidic than the anatase TiO_2, has an obvious adverse effect on the PO production. The results also give strong evidence that the six-coordinated Ti-OOH (η^2) is the important active intermediate for propylene epoxidation.
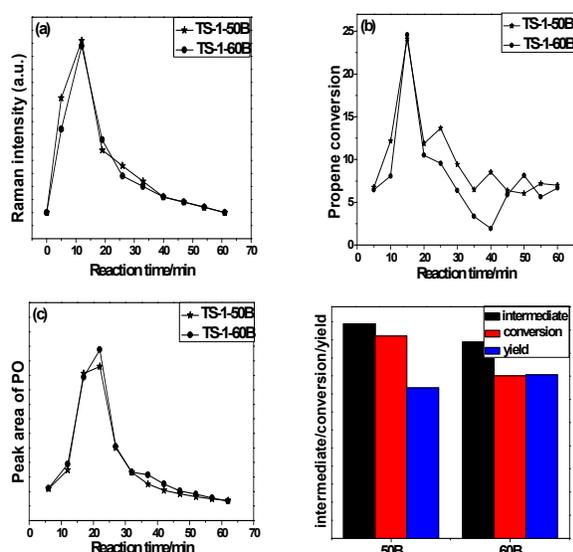
Fig. 12 (A) Raman intensity of the 837 cm^{-1} band (B) the propylene conversion and (C) Peak area of propene oxide in the GC spectra obtained at different times during the epoxidation reaction on the TS-1 with different SiO_2/TiO_2 ratios.
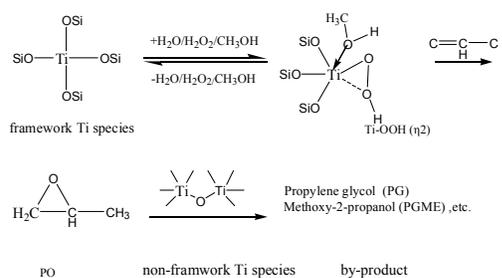
Acknowledgements

Notes and references

1　M. Taramasso, G. Perego and B. Notari, U.S. Patent, 1983, 4410501.
2　B. Notari, Catal. Today., 1993, **18**, 163.
3　G. N. Vayssilov, Catal. Rev. Sci. Eng., 1997, **39**, 209.
4　G. Tozzola, M. A. Mantegazza, G. Ranghino, G. Petrini, S. Bordiga, G. Ricchiardi, C. Lamberti, R. Aulian and A. Zecchina, J. Catal., 1998, **179**, 64.
5　F. Geobaldo, S. Bordiga, A. Zecchina, E. Giamello, G. Leofanti and G. Petrini, Catal. Lett., 1992, **16**, 109.
6　T. Blasco, M. A. Camblor, A. Corma and J. Perez-Pariente, J. Am. Chem. Soc., 1993, **115**, 11806.
7　S. L. Jahn, P. A. P. Nascente and D. Cardoso, Zeolites, 1997, **17**, 416.
8　A. Tual, Zeolites, 1995, **15**, 236.
9　J. Su, G. Xiong, J. C. Zhou, W. H. Liu, D. H. Zhou, G. R. Wang and X. S Wang, J. Catal., 2012, **288**, 1.
10　J. Klaas, G. Schulz-Ekloff and N.I. Jaeger, J. Phys. Chem. B, 1997, **101**, 1305.
11　Stair and P. C. Curr. Opin, Solid State Mater., 2001, **5**, 365.
12　G. Ricchiardi, A. Damin, S. Bordiga, C. Lamberti, G. Spanò, F. Rivetti and A. Zecchina, J. Am. Chem. Soc., 2001, **123**, 11409.
13　C. Li, G. Xiong and Q. Xin, Angew. Chem. Int. Ed., 1999, **38**, 2220.
14　A. Damin, F. Bonino, G. Ricchiardi, S. Bordiga, A. Zecchina and C. Lamberti, J. Phys. Chem. B, 2002, **106**, 7524.
15　M.G. Clerici, G. Bellussi and U.Romano, J. Catal., 1991, **129**, 159.
16　M.G. Clerici, Appl. Catal., 1991, **68**, 249.
17　M. G. Clerici and P. Ingallina, J. Catal., 1993, **140**, 71.
18　A. Zecchina, S. Bordiga, G. Spoto. A. Damin, G. Berlier, F. Bonino, C. Prestipino and C. Lamberti, Top. Catal., 2002, **21**, 67.
19　G. Sankar, J. M. Thomas, C. R. A. Catlow, C. M. Barker, D. Gleeson and N. Kaltsoyannis, J. Phys. Chem. B, 2001, **105**, 9028.
20　C. M. Barker, D. Gleeson, N. Kaltsoyannis, C. R. A. Catlow, G. Sankar and J. M. Thomas, Phys. Chem. Chem. Phys., 2002, **4**, 1228.
21　J. M. Thomas and G. Sankar, Acc. Chem. Res., 2001, **34**, 571.
22　G. Tozzola, M. A. Mantegazza, G. Ranghino, G. Petrimi, S. Bordiga, G. Ricchiardi, C. Lamberti, R. Zulian and A. Zecchina, J. Catal., 1998, **179**, 64.
23　W. Y. Lin, H. Frei, J. Am. Chem. Soc. 2002, **124**, 9292.
24　L.L. Wang, G. Xiong, J. Su and P. Li, J. Phys. Chem. C., 2012, **116**, 9122.
25　S. Bordiga, F. Bonino, A. Damin and C. Lamberti, Phys. Chem. Chem. Phys., 2007, **9**, 4854.
26　W. Panyaburapa, T. Nanok and J. Limtrakul, J. Phys. Chem. C, 2007, **111**, 3433.
27　D. H. Wells, Jr., W. N. Delgass and K. T. Thomson, J. Am. Chem. Soc., 2004, **126**, 2956.
28　P. E. Sinclair and C. R. A. Catlow, J. Phys. Chem. B, 1999, **103**, 1084.
29　J. Klaas, K. Kulawik, G. Schulz-Ekloff and N. I. Jaeger, Stud. Surf. Sci. Catal., 1994, **84**, 2261.
30　F. Z. Zhang, X. W. Guo and X. S. Wang, Catal. Lett., 2001, **72**, 3.
31　G. Li, X. S. Wang and X. W. Guo, Mater. Chem. Phys., 2001, **71**, 195.
32　Wang, L. Q. Study on the Synthetic Process of Titanium Silicalite and Its Catalytic and Oxidation Performance. Ph.D. Thesis, Dalian University of Technology, Dalian, China, 2003.
33　J. Su, J. Zhou, C. Liu, X. Wang and H. Guo, Chin. J. Catal., 2010, **31**, 1995.
34　P. Jeske, G. Haselhorst, T. Weyhermuller, K. Wieghardt and B. Nuber, Iorg. Chem., 1994, 33
35　R. R. Sever and T. W. Root, J. Phys. Chem. B, 2003, **107**, 4080.
36　G. Bellussi, A. Carati, M. G. Clerici, G. Maddinelli and R. Millini, J. Catal., 1992, **133**, 220.
37　W. B. Fan, R. G. Duan, Toshiyuki Yoshiyuki, J. Am. Chem. Soc., 2008, **130**, 10150.
38　D. R. C. Huybrechts, P. L. Buskens, P. A. Jacobs, J. Mol. Catal., 1992, **71**, 129.
39　V. Russo, R. Tesser, E. Santacesaria, and M. Di Serio, Ind. Eng. Chem. Res. 2013, **52**, 1168.